01

Nonlinear electromagnetic response of graphene in tight binding model

© M.V. Davidovich

Saratov National Research State University,
410012 Saratov, Russia
e-mail: davidovichmv@yandex.ru

Received December 25, 2025
Received December 25, 2025
Accepted December 25, 2025

We consider the linear and nonlinear response of a weighted graphene sheet upon incident of a plane electromagnetic wave in the form of a quasi-monochromatic pulse with harmonic filling. The generation of odd harmonics in the reflected and transmitted spectra with a third harmonic generation coefficient of the order of 10-3 is shown.

Keywords: graphene, Schrodinger equation, strong coupling model, kinetic Boltzmann equation, harmonic generation.

DOI: 10.61011/TP.2026.05.63514.338-25

Introduction

Graphene is usually associated as a truly two-dimensional $2D$ material, which was first considered in the approximation of the strong coupling model for the two-dimensional stationary Schrödinger equation (SE) using the periodic potential of two periodic sublattices of carbon atoms in [1]. Graphene band structure has a shape of two converging $\pi^{\pm}$ subbands with energies as $E^{\pm}(\mathbf{q}) = \big(\varepsilon_{2p} \pm \gamma_0 w(\mathbf{q})\big)/(1 \mp \gamma_1 w)$ $\approx \pm\gamma_0 w(\mathbf{q}) + \gamma_1\gamma_0 w^2(\mathbf{q}) + \varepsilon_{2p}$ [2–6]. Here, the bond energy (nearest-neighbor overlap energy) $2.5 \le \gamma_0 \le 3$, [eV], is significantly larger than the overlap integral $\gamma_1 < 0.1$ eV, $\varepsilon_{2p} \approx 0$. Constants are determined from experiment, or from the first principles of calculations (usually the method of density functional theory). Assuming that $\gamma_1 = 0$, we get a symmetric structure of Brillouin zone (BZ) [5] (see also [1–14]):

$$w(\mathbf{q}) = \sqrt{1 + 4\cos(q_x a\sqrt{3}/2)\cos(q_y a/2) + 4\cos^2(q_y a/2)}. \quad (1)$$

The $E(\mathbf{q}) = \pm\gamma_0 w(\mathbf{q})$ dispersion equation (DE) relates the energy of the longitudinal motions of quasi-particles in graphene plane to the two-dimensional quasi-momentum $\mathbf{p}_{\perp} = \mathbf{p} = \mathbf{q}\hbar$, therefore we also denote $w(\mathbf{q}) = w(\mathbf{p}) =$ $= w(p_x, p_y)$ and similarly for other functions. The bond constant $\gamma_0 \approx 3$ eV is significantly larger than the overlap integral $\gamma_1 \sim 0.1$ eV, which is usually neglected. In (1) $a = \sqrt{3}b = 0.246$ nm — lattice constant, $b = 0.142$ nm — spacing between the nearest atoms [1–14]. Some papers mention the spread of the constant γ_0 from 2.5 to 3 eV. Apart from Wallace (1947) study, the band structure was obtained by McClure (1957), as well as by Slonczewski and Weiss (1958). Given that γ_1, we get an assymetric BZ with an energy

$$E(\mathbf{q}) = \pm\gamma_0 w(\mathbf{q})/(1 \mp \gamma_0 w) \approx \pm\gamma_0 w(\mathbf{q}) + \gamma_1\gamma_0 w^2(\mathbf{q}) \text{ [4,15]}.$$

This is a more complicated task and is not reviewed here. In the center of BZ the function (1) is equal to three. In Dirac points

$$\mathbf{q}_{\mathrm{D}} = \mathbf{K} = \big(2\pi/(3\sqrt{3}a),\ 2\pi/(\sqrt{3}a)\big) \quad \text{and} \quad w\big(\mathbf{q}_{\mathrm{D}}^{(\prime)}\big) = 0.$$

When the axes rotate by $\pi/2$ it is required to replace $q_x \leftrightarrow q_y$, whereas the coordinates of Dirac points $\mathbf{q}_{\mathrm{D}} = \mathbf{K}^{(\prime)}$ also change [1–14]. In numerous works (see [2–16] and the literature therein), the Brillouin zone of graphene Fig. 1, *a,b* is presented as a dispersion surface, and its linear properties are also described. In particular, the linear dynamic conductivity of graphene $\hat{\sigma}(\omega, k_x, k_y)$ under the influence of a plane electromagnetic wave $\mathbf{E}(\mathbf{r}, t) = \mathbf{E}_0 \exp\big(-i(\omega t - \mathbf{kr})\big)$ is considered.

We take Maxwell's equations for a plane wave in the form

$$\mathbf{H} = \nabla \times \mathbf{A},\ \ \mathbf{E} = -\mu_0\partial_t\mathbf{A} + (\partial_t\varepsilon_0)^{-1}\nabla\nabla\cdot\mathbf{A}.$$

Let's introduce the impedance $\eta_0 = \sqrt{\mu_0/\varepsilon_0}$. The band structure (1) is obtained by diagonalization of $2D$-Hamiltonian

$$H(\mathbf{q}) = \begin{pmatrix} 0 & h(\mathbf{q}) \\ h^*(\mathbf{q}) & 0 \end{pmatrix}, \quad (2)$$

where

$$h(\mathbf{q}) = \gamma_0\big[\exp(iq_x a) + 2\exp(-iq_x a/2)\cos(q_y a\sqrt{3}/2)\big].$$

We assume $\gamma_0 = 3$ eV, i.e. Fermi velocity

$$v_F = \sqrt{3}\gamma_0 a/(2\hbar) = 0.9739 \cdot 10^6 \text{ m/c}.$$

In the proximity of Dirac points $h(\mathbf{p}) = v_F[ip_x - p_y]$. The action of an electromagnetic wave means adding the term $-e\eta_0\mathbf{A}/c$ to the Hamiltonian in the form of replacing the momentum operator $\hat{\mathbf{p}}$ with $\hat{\mathbf{p}} - e\eta_0\mathbf{A}/c$ (here $e = 1.6 \cdot 10^{-19}$C is a positive charge). For the harmonic fields $\mathbf{E} = i\omega\eta_0\mathbf{A}/c$, from which it follows that $\hat{\mathbf{p}} + ie\mathbf{E}/\omega$ operator will be introduced.

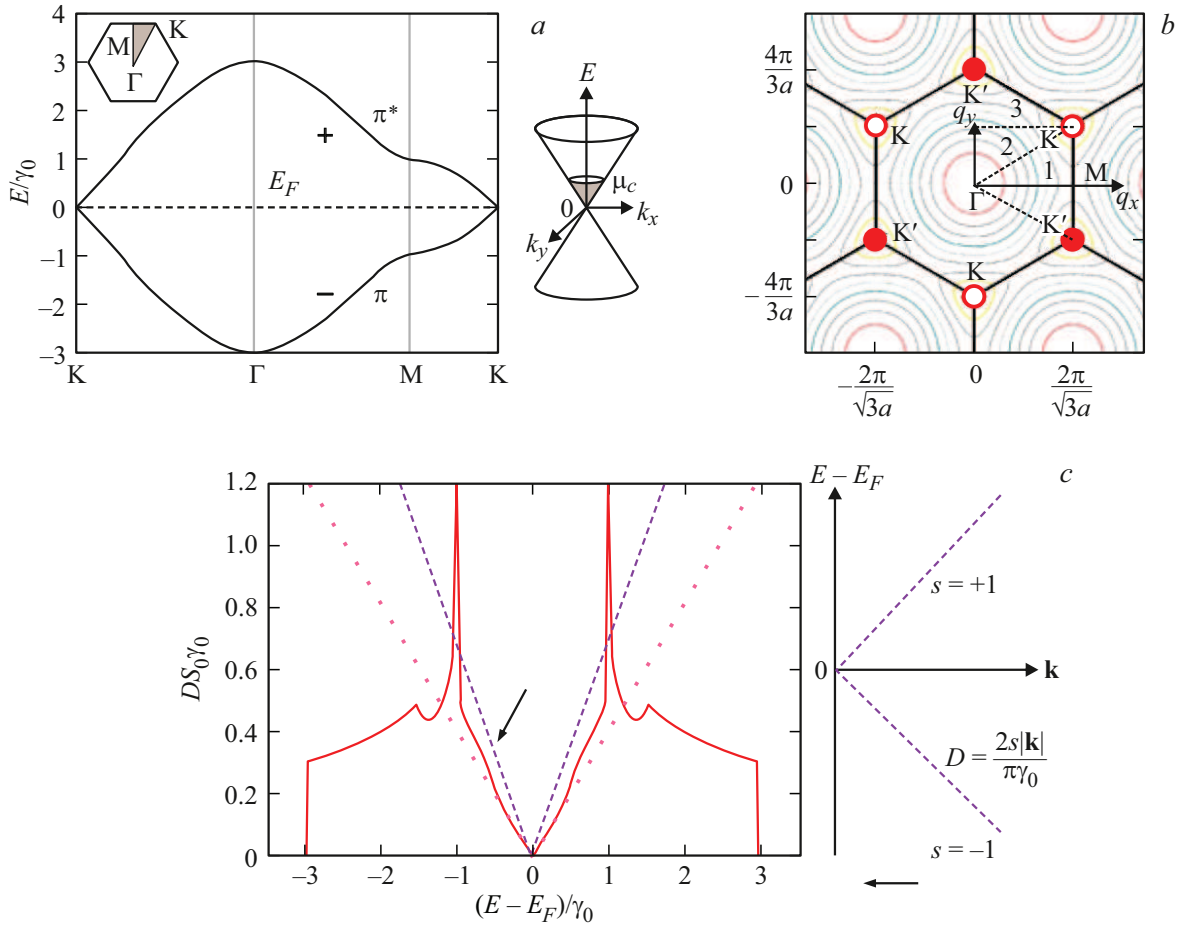

Figure 1. Two-dimensional band structure of graphene (a) with level lines (b) and density of states per cell S_0 at zero temperature (c). Dashed line — linear model.

The conductivity of graphene is usually considered as a linear response to an electric field **E** in the Kubo–Greenwood model using the temperature Green's functions (GF) formalism [8]. At finite temperature, graphene interacts with the thermal field as with a large thermostat, has no „pure“ states, and is described by a density matrix $\hat{\rho}$, satisfying the Liouville– von Neumann [17] equation $i\hbar\partial_t\hat{\rho}(t) = \left[\hat{H}(t), \hat{\rho}(t)\right]$, rather than by a wave function and SE. It is convenient to assume that in the initial state before the field influence the matrix is diagonal $\hat{\rho}(t_0) = \hat{\rho}_0$ with elements

$$f^{\pm}(t_0) = f_0\left(\varepsilon_n(\mathbf{p}^{\pm})\right),$$

where

$$f^{\pm}(t_0) = f_0^{\pm}(\mathbf{q}) = \left[1 + \exp\left(\pm\left(\tilde{\gamma}w(\mathbf{q}) - \tilde{\mu}\right)\right)\right]^{-1}$$

— function of Fermi–Dirac (FDF) that has dimensionless constants $\tilde{\gamma} = \gamma_0/(k_B T)$, $\tilde{\mu} = \mu_c/(k_B T)$. In the first approximation, its diagonal elements contain perturbed distribution functions $f^{\pm}(t)$ of subbands $\pi^{\pm}$. For the current density operator in graphene we have [8]:

$$\hat{j}_\alpha = -e\langle\mathbf{q}'|\hat{v}_\alpha(\mathbf{q}', \mathbf{q})|\mathbf{q}\rangle - e^2\eta_0\langle\mathbf{q}'|\hat{m}^{-1}_{\alpha\beta}(\mathbf{q}', \mathbf{q})|\mathbf{q}\rangle A_\beta. \quad (3)$$

Here, the velocity operator has the following components

$$\hat{v}_\alpha = \partial H(\mathbf{p})/\partial p_\alpha = \gamma_0\hbar^{-1}\partial w(\mathbf{q})/\partial q_\alpha,$$

and inverse operator of the mass tensor is expressed as

$$\left[m^{\pm}_{\alpha\beta}(\mathbf{q})\right]^{-1} = \pm(\gamma_0/\hbar^2)\partial_{q_\alpha}\partial_{q_\beta} w(\mathbf{q}),$$

$m_{\alpha\beta}$ — components of the mass tensor ($\alpha, \beta = x, y$). The value (3) is taken in the interaction representation. In the absence of interaction, the averaging of velocities

$$v^{\pm}_\alpha(\mathbf{q}) = \pm\gamma_0(\partial/\partial q_\alpha)w(\mathbf{q})/\hbar$$

in BZ subbands with equillibrium FDF gives zero, i.e. full average current $\langle\hat{j}_\alpha\rangle$ is absent. When a disturbance is applied from the moment t_0 to the moment t, the system is described by a density matrix. We further assume $t_0 = 0$. The nonlinear current density should be taken in the form of [8,14]: $j_\alpha = j^+_\alpha(t) + j^-_\alpha(t)$,

$j_\alpha^\pm(t) = j_{0\alpha}^\pm(t) + j_{1\alpha}^\pm(t)$, where

$$j_\alpha^\pm(t) = \frac{-2e}{(2\pi)^2}\int\limits_{BZ} v_\alpha^\pm(t,\mathbf{q}) f^\pm(t,\mathbf{q}) d^2q + \frac{-2e^2\eta_0}{(2\pi)^2 c}\int\limits_{BZ}\left[m_{\alpha\beta}^\pm(t,\mathbf{q})\right]^{-1} A_\beta(t) f^\pm(t,\mathbf{q}) d^2q. \quad (4)$$

Here the index $\nu = 0$ of $j_\alpha^\pm(t)$ corresponds to the zeroth degree of the explicitly entering vector potential, and $\nu = 1$ — the first degree, which corresponds to the first and second terms in (4). Also, here $v_\alpha^\pm(\mathbf{q}) = \pm(\gamma_0/\hbar)\partial_{q_\alpha} w(\mathbf{q})$ — the component of group velocity in the subbands $\pi^\pm$.

Linear response of an infinite graphene sheet lying in the $z = 0$ plane to a monochromatic wave

$$\mathbf{E}(t,\mathbf{r}) = \mathbf{E}_0(\omega_0\mathbf{k})\cos(\omega_0 t - \mathbf{kr}) \quad (5)$$

is given in the form of surface current density (hereinafter the word density will be omitted) in the form $j_\alpha(\omega,x,y) = \sigma_{\alpha\beta}(\omega,\mathbf{k})E_\beta(\omega,x,y,0)$, $\alpha,\beta = x,y$, where [8]:

$$\sigma_{\alpha\beta}(\omega,\mathbf{k}) = \frac{ie^2}{\pi^2\hbar}\left\{\sum_{n=1,2}\int\limits_{BZ}\frac{d^2p v_\alpha v_\beta\left\{f_0\left(\varepsilon_n(\mathbf{p}^-)\right) - f_0\left(\varepsilon_n(\mathbf{p}^+)\right)\right\}}{\left[\varepsilon_n(\mathbf{p}^+) - \varepsilon_n(\mathbf{p}^-)\right]\left((\omega - i\omega_c)\hbar - \varepsilon_n(\mathbf{p}^+) + \varepsilon_n(\mathbf{p}^-)\right)}\right.$$
$$\left. + 2\omega\hbar\int\limits_{BZ}\frac{d^2p v_\alpha^{12} v_\beta^{21}\left\{f_0\left(\varepsilon_1(\mathbf{p}^-)\right) - f_0(\varepsilon_2(\mathbf{p}^+))\right\}}{[\varepsilon_2(\mathbf{p}^+) - \varepsilon_1(\mathbf{p}^-)]((\omega - i\omega_c)^2\hbar^2 - [\varepsilon_2(\mathbf{p}^+) - \varepsilon_1(\mathbf{p}^-)]^2)}\right\}. \quad (6)$$

In (6)

$$f_0(\varepsilon) = \left[1 + \exp\left((\varepsilon - \mu_c)/(k_B T)\right)\right]^{-1},$$

$$\varepsilon_n(\mathbf{p}) = \varepsilon_n(\hbar\mathbf{q}) = (-1)^n\left(\gamma_0 w(\mathbf{q}) - \mu_c\right), \quad n = 1$$

stands for the valence band (VB) π^-, $n = 2$ corresponds to the conduction band (CB) π^+, velocity components $v_\alpha^\pm(\mathbf{q}) = \pm\gamma_0(\partial/\partial q_\alpha)w(\mathbf{q})/\hbar$, $\mathbf{p}^\pm = \mathbf{p} \pm \hbar\mathbf{k}/2 = \hbar(\mathbf{q} \pm \mathbf{k}/2)$, i.e. spatial dispersion is taken into account. Specifically,

$$\varepsilon_2(\mathbf{p}^+) - \varepsilon_1(\mathbf{p}^-) = \gamma_0\left[w(\mathbf{q} + \mathbf{k}/2) + w(\mathbf{q} - \mathbf{k}/2)\right] - 2\mu_c,$$

$$\varepsilon_n(\mathbf{p}^+) - \varepsilon_n(\mathbf{p}^-) = (-1)^n\gamma_0\left[w(\mathbf{q} + \mathbf{k}/2) - w(\mathbf{q} - \mathbf{k}/2)\right],$$

$$f_0\left(\varepsilon_n(\mathbf{p}^\pm)\right) = \left[1 + \exp\left((-1)^n\left(\gamma_0 w(\mathbf{q} \pm \mathbf{k}/2) - \mu_c\right)/(k_B T)\right)\right]^{-1}.$$

Here the integration is carried out over the entire BZ. The formula (6) is obtained as a linear response in the Kubo approximation using temperature GF and the Matsubara technique by averaging over the Gibbs ensemble, and only the proportional term $\mathbf{A}$ in the expression for the current operator is taken into account. In IR and THz bands, the spatial dispersion and anisotropic properties of graphene are not very significant [18], therefore scalar conductivity $\sigma(\omega)$ [7] is often used. [8] also gives simplified formulae following from (6). For the ultraviolet band with quanta $\hbar\omega \geq \gamma_0$, σ bonds break, and graphene can be described as a plasma layer [19]. The first term in the tensor(6) corresponds to the intraband conductivity, and the second term corresponds to the interband conductivity. The tensor (6) acts on the spectral amplitude $E_\beta(\omega,x,y,0)$ of the electric field on graphene. If the planar wave has an amplitude E_0 and polarization along x axis, then, in (3) $E_{0x} = E_0 k_z/\sqrt{k_x^2 + k_z^2}$, $E_{0z} = E_0 k_x/\sqrt{k_x^2 + k_z^2} = E_0 k_x/k_0$. Let's denote $\tilde{k} = k_x/k_0 = \sqrt{1 - (k_x/k_0)^2}$. Since $k_y = 0$, the spatial dispersion is determined only by the component k_x, and under monochromatic exposure in a weak field there is a linear response

$$j_x(\omega,x,y) = \sigma_{xx}(\omega,k_x)E_x(\omega,k_x x,y,0) = \sigma_{xx}(\omega,k_x)E_0\tilde{k},$$

where full field is denoted. When plasmons propagate, the spatial dispersion (SD) is determined by all components. For a plane wave, we may write the complex amplitude

$$\dot{\mathbf{E}}(t,\mathbf{r}) = \mathbf{E}_0(\omega_0\mathbf{k})\exp\left(-i(\omega_0 t - \mathbf{kr}/c)\right).$$

In case of normal incidence no SD arises.

1. Problem formulation

Let a plane quasi-monochromatic wave fall from infinity ($z = -\infty$) onto an infinite graphene sheet located at $z = 0$. The full field consists of incident and diffracted fields with components

$$E_x(z,t) = E_x^{in}(z,t) + E_x^d(z,t),$$

$$H_y(z,t) = H_y^{in}(z,t) + H_y^d(z,t),$$

where

$$E_x^{in}(z,t) = E_0\,\Pi(t,z)\cos\left(\omega_0(t - z/c)\right), \quad (7)$$

$$H_y^{in}(z,t) = E_0\,\Pi(t,z)\cos\left(\omega_0(t - z/c)\right)/\eta_0. \quad (8)$$

We use the frequency dependence $\exp(-iEt/\hbar) = \exp(-i\omega t)$, which is commonly used in quantum mechanics. In (7) and (8), the rectangular pulse form factor $\Pi(t,z) = \left[\chi(t - z/c) - \chi(t - \tau - z/c)\right]$, moving at the speed of light c, is used. Here, $\chi(t)$ — is the Heaviside function. In a number of formulas $\chi(t)$ will be omitted, implying its presence. The equations (7), (8) correspond to the fact that at the moment $t = 0$ an incident wave packet (pulse) approached graphene, and at this moment current excitation and reflection begin. At this moment, the volumetric current density $\mathbf{j} = \mathbf{x}_0 J_x(t)\delta(z)$ on graphene is zero, where $J_x(t)$ is the surface current density, i.e. there is no diffraction at $t \leq 0$. For the considered incident wave, the vector potential $\mathbf{A} = -\mathbf{x}_0 c\,\partial_t^{-1} E_x/\eta_0$ can be introduced. We mean the difference between the form factor and the

envelope, which is always smooth. In the non-stationary electrodynamics we have GF as

$$G(\mathbf{r},t)=\frac{1}{2\pi}\int\limits_{-\infty}^{\infty} g(\mathbf{r},\omega)\exp(-i\omega t)d\omega=\frac{1}{4\pi|\mathbf{r}|}\,\delta(t-|\mathbf{r}|/c), \tag{9}$$

$$g(\mathbf{r},\omega)=\frac{1}{(2\pi)^3}\int\limits_{-\infty}^{\infty}\int\limits_{-\infty}^{\infty}\int\limits_{-\infty}^{\infty}\frac{\exp(i\mathbf{kr})}{\mathbf{k}^2-k_0^2}\,d^3k=\frac{1}{4\pi|\mathbf{r}|}\exp(ik_0|\mathbf{r}|). \tag{10}$$

It integrally relates the vector potential $\mathbf{A}$ to the current density $\mathbf{j}(x,y,z,t)$. For the 2D case $\mathbf{j}(x,y,z,t)=\mathbf{J}(x,y,t)\delta(z)$. If there is no dependence on the two coordinates, then the GF will take the form $G(z,t)=c\chi\big(t-|z|/c\big)/2$ with its spectral value $g(z,\omega)=-ic\exp(-i\omega|z|/c)/(2\omega)$. This GF satisfies the equation $(\partial_z^2+k_0^2)G(z,t)=-\delta(z)$. The component of the diffracted field is determined in terms of the vector potential $\mathbf{x}_0 A_x^d(z,t)$:

$$A_x^d(z,t)=\int\limits_{-\infty}^{\infty}dt'\int\limits_{-\infty}^{\infty}G(z-z',t-t')j_x(z',t')dz'$$

$$=\frac{c}{2}\int\limits_{0}^{\infty}\chi(t-t'-|z|/c)J(t')dt', \tag{11}$$

$J(t)=J_x(t)$ — surface current density. Integral (11) may be written from 0 to $t-|z|/c$. Consequently, $\partial_t A_x^d(z,t)=cJ(t-|z|/c)/2$. For the incident field, we have a vector potential

$$A_x^{in}(z,t)=-\frac{cE_0\Pi(z,t)}{\eta_0\omega_0}\sin\big(\omega_0(t-z/c)\big). \tag{12}$$

Obviously, this result can also be obtained from spectral GF if we take $j_x(\mathbf{r},\omega)=J(\omega)\delta(z)$, determine $J(\omega)$, and then reverse the result by Fourier. This allows to get the fields (7), (8). After differentiation (11) we'll find the components:

$$E_x^d(z,t)=-\eta_0 J(t-|z|/c)/2, \tag{13}$$

$$H_y^d(z,t)=-\mathrm{sgn}(z)J(t-|z|/c)/2, \tag{14}$$

as well as their ratio $E_x^d(z,t)/H_y^d(z,t)=\mathrm{sgn}(z)\eta_0$. The diffracted wave goes in both directions and is determined by the current density to be found. For the full field we have

$$E_x(0,t,k_x)=E_0\tilde{k}\cos(\omega_0 t)$$

$$-\frac{\eta_0}{2}\int\limits_{0}^{t}\Sigma_{xx}(t-t',k_x)E_x(0,t',k_x)dt',$$

where $\Sigma_{xx}(t,k_x)$ — some operator, generally speaking, intergal and non-linear in E_0. The field excites the current $j_x(t,k_x)$. Since all quantities are determined at a certain point in time, their spectra are instantaneous, i.e. they depend on time. The current determined by the conductivity has the following form

$$j_{1x}(t,k_x)=\frac{1}{2\pi}\int\limits_{-\infty}^{\infty}\exp(-i\omega t)\sigma_{xx}(t,\omega,k_x)E_x(t,\omega,k_x)d\omega.$$

Here $\sigma_{xx}(t,\omega,k_x)$ — is the instantaneous spectrum of total conductivity, and in the general case it defines an integral operator of the form

$$j_{1x}(t,k_x)=\int\limits_{0}^{t}\Sigma_{xx}(t-t',k_x)E_x(0,t',k_x)dt'.$$

This leads to the need to solve nonlinear equations. In the incident field approximation, it can be considered quasi-monochromatic, with $E_x(\omega)=-i\omega\eta_0 A_x(\omega)/c$.

We consider a long-term exposure, i.e. assume that t is infinitely large. Then, in the quasi-monochromatic process, this density in the continuous spectrum contains the fundamental and higher harmonics of the carrier frequency ω_0 plus a small continuous spectrum. At $z=0$ the electrical field is continuous, from where

$$E_x^{in}(-0,t)+E_x^{in}(-0,t)=E_x^{in}(+0,t)+E_x^{in}(+0,t).$$

This ratio is fulfilled automatically. At $z=0$ the magnetic field has a jump

$$H_y^d(+0,t)-H_y^d(-0,t)=-J(t)=2E_x^d(0,t)/\eta_0.$$

If the field is active for a very long time, the process can be considered periodic, and then at $t>0$

$$J(t)\approx J_1\cos(\omega_0 t)+J_3\cos(3\omega_0 t)+J_5\cos(5\omega_0 t)+\ldots.$$

In reality, there are peaks at these frequencies on the continuous $J(\omega)$ spectrum. By introducing the reflection coefficient over the electric field as $R(t)=-\eta_0 J(\omega_0 t)\cos(\omega_0 t)/(2E_0)$ for the first harmonic, we have $R_1(t)=-\eta_0 J_1/(2E_0)$. Neglecting the other harmonics, due to the continuity for the transmission coefficient, we have $1+R_1=T_1$. Obviously, it is possible to introduce harmonic transformation coefficients $R_n=T_n=-\eta_0 J_n/(2E_0)$. The obtained ratios are not sufficient to determine the current density $J(t)$. In the linear case, such an additional relation is the $J(\omega)=\sigma(\omega)E_x(\omega)$ coupling, which leads to the equation

$$E_x(\omega)=J(\omega)/\sigma(\omega)=i\omega\eta_0\big[A_x^{in}(\omega)+A_x^d(\omega)\big]/c,$$

which, given $A_x^d(\omega)=icJ(\omega)/(2\omega)$, defines the current density

$$J(\omega)=\frac{i\omega\eta_0\sigma(\omega)A_x^{in}(\omega)/c}{1+\eta_0\sigma(\omega)/2}. \tag{15}$$

In the non-stationary case, to determine the current density, an integral equation in the time domain should be

solved, which is also nonlinear when taking into account nonlinear terms.

Graphene — is a highly nonlinear material. Its nonlinear properties have been studied in a large number of papers. Most studies, e.g., [20–36], use the quantum electrodynamics (QED) model of massless Dirac fermions in the linear dispersion approximation $E(\tilde{\mathbf{q}}) = \pm\hbar|\tilde{\mathbf{q}}|v_F$ with valley degeneracy $g_v = 2$ and spin degeneracy $g_x = 2$, where the Fermi velocity is $v_F = \sqrt{3}\gamma_0 a/(2\hbar) = 0.974 \cdot 10^6$ m/s (at $\gamma_0 = 3$ eV). In this model, $\tilde{\mathbf{q}} = \mathbf{q} - \mathbf{q}_D$ wavenumber and energy are calculated from zero Fermi level (FL) corresponding to the two Dirac points $\mathbf{K}$ and $\mathbf{K}'$ (Fig. 1, 2). The formal similarity with QED when a strong field acts on the quantum vacuum has led to many studies on non-perturbative methods for determining the production of quasiparticle pairs such as the Schwinger effect [29,30] or tunneling of Landau–Zener [36]. It should be noted that graphene differs significantly from the quantum vacuum. At Dirac points, the density of states D is zero, as is the effective mass (Fig. 2), and when displaced from them, a nonzero effective mass appears, which calls into question the accuracy of models of massless fermions. The particles can be located not only in valleys (Dirac cones), but also in the vicinity of BZ center, so estimating their number from the density of states (DOS) of the massless model leads to their overestimation (in Fig. 1, *c* linear DOS is higher than real DOS). QED uses electrical neutrality, which for distribution functions (DF) is interpreted as the electrical neutrality of the electronic and hole subsystems $f(\mathbf{p}, t) = f_e(\mathbf{p}, t) = f_h(\mathbf{p}, t)$ [36]. In fact, this is not the case: for graphene $f(\mathbf{p}, t) = f_e(\mathbf{p}, t) = 1 - f_h(\mathbf{p}, t)$ [1,4] (at $\mu_c = 0$), which corresponds to the conservation of the number of particles (the main normalization condition in quantum mechanics). At zero temperature in pure graphene, the conduction band (π^+ or π^*) is empty [1], all electrons are in the valence band (VB), and electrical neutrality is provided by carbon ions in the lattice. In addition, these papers consider strong and nonstationary fields applied to graphene together with linear dispersion.

We consider the following nonlinear effects that determine the nonlinear response of graphene. Let's assume that the field is not very strong (no heating), i.e. not resulting in heating of carriers and variation of temperature and changes in the number of particles in the subbands, let alone, not resulting in any break of σ-bonds. Such a break occurs in fields of the order of 10^{10} V/m, and also in the presence of $\omega\hbar > \gamma_0$ quanta, which can occur under the influence of a strong and very short pulse. Then the plasma layer model [19] should be used for conduction. The condition $\omega\hbar < \gamma_0$ denotes the wave packets with a limited spectrum. For such a limitation, smooth form factors can be used instead of rectangular ones. We consider a quasi-periodic field that operates for a long time and does not strongly distort the Brillouin zone. Formally, we consider the Brillouin zone distortion by replacing the quasi-momentum in (1) with $\mathbf{p} - \eta_0 e\mathbf{A}(t)/c$ or $q_x \to q_x - q_0(t)$, $q_0(t) = e\eta_0 A_x(t)/(\hbar c)$. Let's assume,

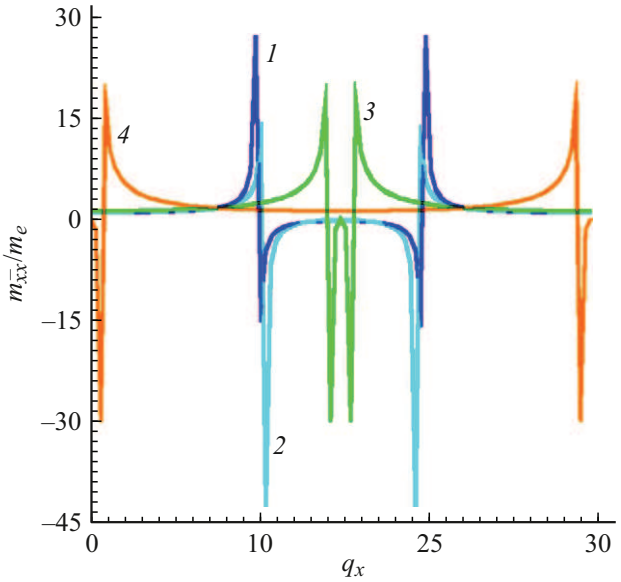

Figure 2. Normalized effective mass $m_{xx}^-(\mathbf{q})/m_e$ versus q_x at different q_y: $q_y = 0$ (curve *1*), $q_y = \pi/(3a)$ (*2*), $q_y = 2\pi/(3a)$ (*3*), $q_y = 4\pi/(3a)$ (*4*). The peaks correspond to the poles. In the vicinity of Dirac points the tendency to zero is almost linear (curve *3*, $q_x = 2\pi/(\sqrt{3}a)$, curve *4* at $q_x = 0$ and $q_x = 4\pi/(\sqrt{3}a)$). Range of values q_x: $\left(0, 4\pi/(\sqrt{3}a)\right)$, $\delta = 0$, $\varepsilon = 0$.

that averaged over a period „addition“ $\langle q_0 \rangle$ is significantly less than $\langle q_x \rangle$ averaged over the Brillouin zone. At the moment t_0 of disturbance action, the system is described by a diagonal density matrix, which includes undisturbed DF subbands. We assume that the matrix retains a diagonal form, i.e. we neglect the non-diagonal terms. DF satisfy the kinetic Boltzmann equations (KBE), which are solved in the Bhatnagar–Gross–Krook (BGK) approximation. It should be noted that over the small parameter $q_0(t)$ are expanded both as a dispersion (1) and as included in (4) components of the group velocities, the effective mass tensor, and DF. The mentioned expansions are expressed as

$$w(t, \mathbf{q}) = w(\mathbf{q}) + w_1(\mathbf{q})q_0(t) + w_2(\mathbf{q})q_0^2(t) + w_3(\mathbf{q})q_0^3(t),$$

$$v^{\pm}(t, \mathbf{q}) = \pm v_F\left[v_0(q) + v_1(q)q_0(t) + v_2(q)q_0^2(t) + v_3(q)q_0^3(t)\right],$$

$$f^{\pm}(t, \mathbf{q}) = f_0^{\pm}(t, \mathbf{q}) + f_1^{\pm}(\mathbf{q})q_0(t) + f_2^{\pm}(\mathbf{q})q_0^2(t) + f_3^{\pm}(\mathbf{q})q_0^3. \tag{16}$$

They are given in the Appendix (formulae (A1)–(A14)). We limit the terms to the third order, which allows us to obtain the third harmonic. Since

$$\left[m_{\alpha\beta}^{\pm}(t, \mathbf{q})\right]^{-1} A_\beta(t) = \left[m_{xx}^{\pm}(t, \mathbf{q})\right]^{-1} A_x(t)$$
$$= \pm c\gamma_0\left[\partial_{q_x}^2 w(t, \mathbf{q})\right]^{-1} q_0(t)/(e\eta_0\hbar),$$

then, we have

$$\left[m_{xx}^{\pm}(t,\mathbf{q})\right]^{-1}A_x(t)=\frac{\pm c}{e\eta_0\hbar w''(\mathbf{q})}$$
$$\times\left[q_0(t)-\frac{w_1''(\mathbf{q})}{w''(\mathbf{q})}q_0^2(t)+\left(\frac{w_1''^2(\mathbf{q})}{w''^2(\mathbf{q})}-\frac{w_2'''(\mathbf{q})}{w''(\mathbf{q})}\right)q_0^3(t)\right]. \quad (17)$$

The prime implies a derivative. After integration by BZ in (4), we also leave the terms up to the third order, which allows us to determine the response in the form of the third harmonic. Since we've introduced the wavenumber $q_0(t)=e\eta_0 A_x(t)/(\hbar c)$, then, at $A_x(t)=1\,\mathrm{A}$ its maximal amplitude $q_0(t)\sim 2\cdot 10^9\,\mathrm{m}^{-1}$, while the average value $q_x\sim\pi/a\sim 1.3\cdot 10^{10}\,\mathrm{m}^{-1}$. Albeit q_x varies in BZ from zero, it can be assumed that for $A_x(t)<1\,\mathrm{A/m}^2$, the expansion by $q_0(t)$ parameter is valid. We assume that $e\eta_0 A_x(t)a/c\ll 2\hbar$. At a frequency of $\omega=1\,\mathrm{THz}$ this corresponds to the field intensity $E_0<E_{cr}=1.25\cdot 10^6\,\mathrm{V/m}$.

Writing down the perturbed Hamiltonian $\hat{H}=\hat{H}_0+\delta\hat{H}$, we have the equation for the density matrix $\hat{\rho}(t)=\hat{\rho}_0(0)+\delta\hat{\rho}(t)$:

$$i\hbar\partial_t\left(\hat{\rho}_0(0)+\delta\hat{\rho}(t)\right)=\left[\frac{(\hat{\mathbf{p}}-e\eta_0\mathbf{A}/c)^2}{2m_e}+V_0(x,y),\hat{\rho}_0(0)+\hat{\rho}_1(t)\right],$$

where V_0 — is the periodic potential of graphene, and the undisturbed matrix satisfies the equation

$$i\hbar\partial_t\hat{\rho}_0(0)=\left[\hat{H}_0,\hat{\rho}_0(0)\right]=\hat{H}_0\hat{\rho}_0(0)-\hat{\rho}_0(0)\hat{H}_0=0.$$

For its pertubation we have

$$i\hbar\partial_t\,\delta\hat{\rho}_1(t)=\left[\hat{H}_0,\delta\hat{\rho}(t)\right]$$
$$+\left[\frac{-2e\eta_0\mathbf{A}\hat{\mathbf{p}}/c+e\eta_0\mathbf{A}^2/c^2}{2m_e},\hat{\rho}_0(0)+\delta\hat{\rho}(t)\right] \quad (18)$$

at the initial condition $\delta\hat{\rho}(0)=\hat{0}$. Due to this condition, the first switch is small at short times. $e\eta_0\mathbf{A}^2/c^2$ value in the second switch can be omitted because it switches with matrices. The first term in the second switch gives a linear response to the Kubo model if we take $\delta\hat{\rho}(t)=\hat{\rho}_1(t)$ on the left and omit $\delta\hat{\rho}(t)$ value on the right in the switch.

$$i\hbar\partial_t\hat{\rho}_1(t)=\left[\hat{H}_0,\hat{\rho}_1(t)\right]-\frac{e\eta_0\mathbf{A}}{m_e c}\left[\hat{\mathbf{p}},\hat{\rho}_0(0)\right]. \quad (19)$$

If we leave it, then $\delta\hat{\rho}(t)=\hat{\rho}_1(t)+\hat{\rho}_2(t)$, and for the nonlinear response we have the equation

$$i\hbar\partial_t\hat{\rho}_2(t)=\left[\hat{H}_0,\hat{\rho}_2(t)\right]-\frac{e\eta_0\mathbf{A}}{m_e c}\left[\hat{\mathbf{p}},\hat{\rho}_1(t)+\hat{\rho}_2(t)\right].$$

Since $\hat{\rho}_1(t)$, according to (19), is proportional to $\mathbf{A}\cdot[\hat{\mathbf{p}},\hat{\rho}_0(0)]$, this is a nonlinear equation. The matrix $\hat{\rho}_1(t)$ is already off-diagonal. If, however, the off-diagonal elements are small, the averaging with the $\hat{\rho}(t)$ matrix can be replaced by the averaging with FR $f^{\pm}(t)$.

In case of a stationary SE solution for graphene, the Bloch wave function consists of two sublattice wave functions:

$$\psi(\mathbf{r})=\sum_{R_A}\psi_A(\mathbf{R}_A)\varphi(\mathbf{r}-\mathbf{R}_A)+\sum_{R_B}\psi_B(\mathbf{R}_B)\varphi(\mathbf{r}-\mathbf{R}_B),$$

where vectors $\mathbf{R}_A=n_A\mathbf{a}+n_B\mathbf{b}+\boldsymbol{\tau}_1$ and $\mathbf{R}_B=n_A\mathbf{a}+n_B\mathbf{b}$ at integer values n_A and n_B, $\mathbf{a}$ and $\mathbf{b}$ — are the translation vectors.

$$\mathbf{a}=a(1,0),\quad \mathbf{b}=a(-1/2,\sqrt{3}/2),\quad \boldsymbol{\tau}_1=a(0,1/\sqrt{3}),$$
$$\boldsymbol{\tau}_2=a(-1/2,-\sqrt{3}/2),\quad \boldsymbol{\tau}_3=a(1/2,-\sqrt{3}/2)\ [2\text{–}8],$$
$$\psi_A(\mathbf{R}_Z)=f_A(\mathbf{q})\exp(i\mathbf{q}\mathbf{R}_A),\ \psi_B(\mathbf{R}_B)=f_B(\mathbf{q})\exp(i\mathbf{q}\mathbf{R}_B),$$
$$H(\mathbf{q})\begin{pmatrix}f_A(\mathbf{q})\\f_B(\mathbf{q})\end{pmatrix}=\begin{pmatrix}0 & h(\mathbf{q})\\h^*(\mathbf{q}) & 0\end{pmatrix}\begin{pmatrix}f_A(\mathbf{q})\\f_B(\mathbf{q})\end{pmatrix}=E(\mathbf{q})\begin{pmatrix}f_A(\mathbf{q})\\f_B(\mathbf{q})\end{pmatrix}.$$

and the subbands energy is expressed as

$$E^{\pm}(\mathbf{q})=\pm\gamma_0\left|\sum_{l=1}^{3}\exp(-i\mathbf{q}\boldsymbol{\tau}_l)\right|.$$

After diagonalization $\hat{H}_0\hat{\rho}_0=\hat{E}\hat{\rho}_0$:

$$\hat{H}_0=\begin{pmatrix}H_{11} & 0\\0 & H_{22}\end{pmatrix},$$
$$\hat{E}=\begin{pmatrix}+\gamma_0 w(\mathbf{q}) & 0\\0 & -\gamma_0 w(\mathbf{q})\end{pmatrix},$$
$$\hat{\rho}_0(0)=\begin{pmatrix}f_0^+(\mathbf{q}) & 0\\0 & f_0^-(\mathbf{q})\end{pmatrix}. \quad (20)$$

At zero temperature and zero chemical potential $f_e(\mathbf{q})=f^-(\mathbf{q})=1$, $f_h(\mathbf{q})=f^+(\mathbf{q})=1-f_e(\mathbf{q})=0$, the electrons completely fill the VB, but there are no particles in the CB. In the general case, for the density of the number of particles, we have

$$n_e(t)=\frac{2}{\Omega S_0}\iint_{BZ}f_e(t,\mathbf{q})d^2q,$$
$$n_h(t)=\frac{2}{\Omega S_0}\iint_{BZ}\left(1-f_e(t,\mathbf{q})\right)d^2q.$$

Here $\Omega=2(2\pi/a)^2/\sqrt{3}$ — $2D$ volume of BZ (Fig. 1), $S_0=\sqrt{3}a^2/2=0.05238\,\mathrm{nm}^2$ — area of hexagon, $\Omega S_0(2\pi)^2$. For pure graphene $n_0=3.8\cdot 10^{19}\,1/\mathrm{m}^2$ corresponds to the two π-electrons per hexagon S_0. The matrix $\hat{\rho}_1(\mathbf{q})$ is off-diagonal, but doesn't depend on coordinates. It is rather difficult to obtain a solution of (18) in general, but in the case of adiabatic inclusion of the interaction during the quasi-monochromatic process for matrix elements of (19) we have

$$(\rho_1)_{mn}\approx\frac{f_0(E_{nn})-f_0(E_{mm})}{i\hbar(\omega+i\omega_c)-E_{mm}+E_{nn}}\frac{e\eta_0\mathbf{A}}{m_e c}\cdot\langle q|\hat{\mathbf{p}}|q\rangle, \quad (21)$$

where $\langle q|\hat{\mathbf{p}}|q\rangle$ — matrix element of quasi-momentum. In our case, $\mathbf{A}=\mathbf{x}_0A_x=\mathbf{x}_0cE_x/(i\omega\eta_0)$, $\hat{\mathbf{p}}=\hbar\mathbf{x}_0\partial_x$, and

formula(21) gives a linear response to the electric field when averaging the current density operator. It can be used as a first approximation for the iterative solution of (18). However, we will not solve this equation, but will consider the density matrix to be diagonal. Hence, we need to solve KBE for DF:

$$\left(\partial_t+\frac{p_x-\hbar q_0(t)}{m_{xx}(t,\mathbf{q})}\,\partial_x+\frac{p_y}{m_{yy}(t,\mathbf{q})}\,\partial_y+F_x\partial_{p_x}+F_y\partial_{p_x}\right)\times f(t,x,y,\mathbf{p})=J_{col}(t,\mathbf{p}). \quad (22)$$

In this equation, $m_{xx}(t,\mathbf{q})$, $m_{yy}(t,\mathbf{q})$ are the components of the effective mass, and $F_x=-eE_x(t)$, $F_y=-eE_y(t)$ are the components of the force acting on the electron. Since on graphene E_x does not depend on coordinates, the initial DF $f_0(\mathbf{q})$ and the collision integral are also independent of coordinates, then the DF can be considered independent of x and y, i.e. assume $\partial_x=0$ and $\partial_y=0$. Thus, we use DF in the momentum representation. In the initial moment $F_y=-eE_y(0)=0$. KBE solution should be obtained as solutions to the Cauchy problem. For the collision integral in BGK approximation and the relaxation time $\tau_r(\mathbf{q})$, we have [4]:

$$J_{col}(t,\mathbf{q})=\frac{f(0,\mathbf{q})-f(t,\mathbf{q})}{\tau_r(\mathbf{q})}.$$

Expansions in $A_x(t)$ are actually a theory of perturbations in time. The purtubation in a quasi-periodic process is small if the amplitude is small. Considering that at the initial moment $q_0(t)=eE_0\cos(\omega_0 t)/(\omega_0\hbar)$, we have an expansion in field amplitude E_0. Functions $w'(\mathbf{q})=w_1(\mathbf{q})$ and $w'''(\mathbf{q})=w_3(\mathbf{q})$ are odd functions in q_x, and $w(\mathbf{q})$ and $w''(\mathbf{q})=w_2(\mathbf{q})$ are even. DF in $\pi^{\pm}$ subbands have the form

$$f^{\pm}(t,\mathbf{q})=\left[1+\exp\left(\frac{\pm\gamma_0\big(w(\mathbf{q})+w_1(\mathbf{q})q_0(t)+w_2(\mathbf{q})q_0^2(t)/2\big)-\mu_c}{k_{\mathrm{B}}T}\right)\right]^{-1}. \quad (23)$$

The signs $\pm$ correspond to $\pi^{\pm}$ subbands. Expanding the exponent

$$\exp(u+\delta)=\exp(u)+\exp(u)\delta+\exp(u)\delta^2/2+\exp(u)\delta^3/6,$$

where the values are designated

$$\delta=\delta_{\pm}(t,\mathbf{q})=\pm\gamma_0\big[w_1(\mathbf{q})q_0(t)/(k_{\mathrm{B}}T)+w_2(\mathbf{q})q_0^2(t)/(2k_{\mathrm{B}}T)\big],$$

$$u=u_{\pm}(\mathbf{q})=\big(\pm\gamma_0\,w(\mathbf{q})-\mu_c\big)/(k_{\mathrm{B}}T),$$

with an accuracy up to $q_0^3(t)$, we get ($\pm$ is neglected)

$$f(t,\mathbf{q})=f(\mathbf{q})+f_1(\mathbf{q})q_0(t)+f_2(\mathbf{q})q_0^2(t)+f_3(\mathbf{q})q_0^3(t). \quad (24)$$

The coefficients are listed in the Appendix. Let's write down this formula also as $f(t,\mathbf{q})=f(\mathbf{q})+\Delta f(t,\mathbf{q})$. Assuming $k_{\mathrm{B}}T\sim 0.026$ eV, i.e. a room temperature. Inside the valence band $f(\mathbf{q})\approx 1$, $\exp\big(u_{\pm}(\mathbf{q})\big)\ll 1$, and the correction is exponentially small: $\Delta f(t,\mathbf{q})=-\exp\big(u_{\pm}(\mathbf{q})\big)\delta(1+\delta/2)$. Inside the conduction band $f(\mathbf{q})\approx\mathbf{0}$, $\exp\big(u_{\pm}(\mathbf{q})\big)\gg 1$, the correction is also exponentially small. If $f(\mathbf{q})=1/2$ (about FL), then $\exp\big(u_{\pm}(\mathbf{q})\big)=1$, and the correction is also small $\Delta f(t,\mathbf{q})=-\delta(1+3\delta/4)/4$. In general,

$$\Delta f(t,\mathbf{q})=q_0(t)f_1(\mathbf{q})+q_0^2(t)f_2(\mathbf{q})+q_0^3(t)f_3(\mathbf{q})$$

is given by the formula (A12).

These formulas can be used without solving KBE, i.e. considering that pertubation of DF occurs only due to the purtubation of the BZ. This simplifies the problem significantly. Considering DF $f^{\pm}$ as diagonal elements of the density matrix satisfying the KBE, we obtain its solution for harmonic excitation. It is convenient to consider it in a complex form. Then for the complex DF we have the following expansion

$$f^{\pm}(t,\mathbf{q})=f^{\pm}(\mathbf{q})+f_1^{\pm}(\mathbf{q})\exp(-i\omega_0 t)+f_3^{\pm}(\mathbf{q})\exp(-3i\omega_0 t),$$

Let's represent the field in terms of odd harmonics.

$$\dot{E}_x=E_0\exp(-i\omega_0 t)+\kappa_{13}E_0\exp(-3i\omega_0 t).$$

The real DF shall be considered as

$$f^{\pm}(t,\mathbf{q})=f^{\pm}(\mathbf{q})+f_1^{\pm}(\mathbf{q})\cos(\omega_0 t)+f_3^{\pm}(\mathbf{q})\cos(3\omega_0 t),$$

where the modules of complex amplitudes are taken. The complex KBE in BGK approximation is written as

$$\left(-i\omega_0 f_1^{\pm}+\frac{eE_0}{\hbar}\nabla_{q_x}f_1^{\pm}(\mathbf{q})\right)\exp(-i\omega_0 t)+\left(-3i\omega_0 f_3^{\pm}+\frac{eE_0\kappa_{13}}{\hbar}\nabla_{q_x}f_3^{\pm}(\mathbf{q})\right)\exp(-3i\omega_0 t)=-\frac{f_1^{\pm}(\mathbf{q})\exp(-i\omega_0 t)+f_3^{\pm}(\mathbf{q})\exp(-3i\omega_0 t)}{\tau_r}. \quad (25)$$

Due to the arbitrariness of time, it splits into two:

$$(-i\omega_0+\omega_c)\dot{f}_1^{\pm}(\mathbf{q})=\frac{eE_0}{\hbar}\,\partial_{q_x}\dot{f}^{\pm}(\mathbf{q}),$$

$$(-3i\omega_0+\omega_c)\dot{f}_3^{\pm}(\mathbf{q})=\frac{e}{\hbar}\,\kappa_{13}E_0\partial_{q_x}\dot{f}^{\pm}(\mathbf{q}).$$

Let's use the approximation

$$\partial_{q_x}\dot{f}^{\pm}(\mathbf{q})\approx\partial_{q_x}f_0^{\pm}(\mathbf{q})=\frac{\hbar v_x^{\pm}}{k_{\mathrm{B}}T}\exp\big(\pm u(\mathbf{q})\big)f_0^{\pm}(\mathbf{q})\big[1-f_0^{\pm}(\mathbf{q})\big].$$

In it $u(\mathbf{q})=\big(\gamma_0\,w(\mathbf{q})-\mu_c\big)/k_{\mathrm{B}}T$. Then, we get the solutions

$$f_1^{\pm}(\mathbf{q})=\frac{eE_0v_x^{\pm}(\mathbf{q})}{k_{\mathrm{B}}T}\exp\big(\pm u(\mathbf{q})\big)\frac{f_0^{\pm}(\mathbf{q})[1-f_0^{\pm}(\mathbf{q})]}{\sqrt{\omega_0^2+\omega_c^2}}, \quad (26)$$

$$f_3^{\pm}(\mathbf{q}) = \frac{eE_0\kappa_{13}v_x^{\pm}(\mathbf{q})}{k_{\mathrm{B}}T}\exp\bigl(\pm u(\mathbf{q})\bigr)\frac{f_0^{\pm}(\mathbf{q})[1-f_0^{\pm}(\mathbf{q})]}{\sqrt{9\omega_0^2+\omega_c^2}}. \tag{27}$$

The collision frequency $\omega_c = 1/\tau_r$ in them, we consider small compared to ω_0. If it is approximate to determine κ_{13}, these relations allow us to refine the third harmonic by taking

$$f^{\pm}(t,\mathbf{q}) = f^{\pm}(\mathbf{q}) + \left(\frac{\omega_0\hbar}{eE_0}\right)q_0(t)f_1^{\pm}(\mathbf{q}) + f_3^{\pm}(\mathbf{q})\left[4\left(\frac{\omega_0\hbar}{eE_0}\right)^3 q_0^3(t) - 3q_0(t)\left(\frac{\omega_0\hbar}{eE_0}\right)\right]. \tag{28}$$

Compared to $f^0(\mathbf{q})$ the value (26) will be small, if $eE_0v_F \ll \omega_0 k_{\mathrm{B}}T$. Taking the frequency $\omega_0 = 10^{13}$ Hz and assuming the relaxation time 10^{-12} s, at room temperature we obtain the fields $E_0 \ll 10^{10}$ V/M. Correction (27) is about $\kappa_{13}/3$ times less. Therefore, if the fields are not too strong and the temperatures are not too low, it is quite possible to take $f^{\pm}(\mathbf{q}) = f_0^{\pm}(\mathbf{q})$. The use of (26)–(28) complicates the result. Considering DF $f_0^{\pm}(t,\mathbf{q})$ in (25) and velocity as perturbed quantities expanded in the complex parameter $\tilde{q}_0(t) = \tilde{q}_0\exp(-i\omega_0 t)$, more complex relations can be obtained that provide for other harmonics. Due to the nonlinearity, the solution of such equations should be obtained iteratively by determining κ_{13} iteratively with consideration for (4).

A strict time-based approach requires a calculation for each response moment (4) with simultaneous solution of the time domain KBE and the problem of excitation of a scattered field by current. The corresponding solutions shall be used in (4). To obtain a harmonic composition, the instantaneous spectra should be calculated for a given time. This approach is very costly: integration in the Brillouin zone should be carried out for each moment in time, and there are a lot of such moments for the quasi-monochromatic process. Integrals in the BZ are not analytically calculated. Therefore, to get a response, it is easier to use the expansions to integrate in the BZ one at a time. Using the expansions makes it easier to get a response in the form of the third harmonic and higher harmonics. If the field is not too strong, the change of DF in the KBE can be ignored, i.e. we only take into account the expansion (A12). We may also ignore the change in A_x due to the action of the current.

2. Numerical results

Graphene should actually be considered as a finite sheet on a dielectric substrate excited by a finite quasi-monochromatic plane pulse, as in the experiments of jcite37-39. In the dispersion of such a sheet, there is an energy slit δ of the order of fractions of eV. For the final sheet, a nonlinear volume-surface integral equation for the field in a dielectric and the current density in graphene should be solved simultaneously, taking into account the above definitions of the type (4) and (18) or (22). At each such moment in time, it is necessary to integrate in the ZB and calculate the response $J(t)$, for which the spectrum should then be determined. For an infinite sheet, it is necessary to determine the response taking into account the diffraction field (11), which is also a nonlinear problem. Nonlinear equations should be solved jointly and iteratively. The numerical implementation of such a process is a very complex and computationally demanding task. It is much easier to use the monochromatic approximation, using the fact that the higher harmonics are small compared to the first one.

Let's consider the response (4). The absence of a field leads to the fact that the first term in (4), when integrated in BZ, turns into zero, as does the second one. This is because the even functions of the variable q_x, and $v_x^{\pm}(0,\mathbf{q})$ — are odd functions. Integrating in the second term in (4) the integral in parts, taking into account

$$\bigl[m_{xx}^{\pm}(t,\mathbf{q})\bigr]^{-1} = \pm\gamma_0\partial_{q_x}^2\, w(t,\mathbf{q})/\hbar^2 = \partial_{q_x}v_x^{\pm}(t,\mathbf{q})/\hbar,$$

let's find

$$\frac{-2e^2\eta_0}{(2\pi)^2 c k_{\mathrm{B}}T}\int\limits_{BZ} A_x(t)v_x^{\pm 2}(t,\mathbf{q})f^{\pm}(t,\mathbf{q})\bigl[1-f^{\pm}(t,\mathbf{q})\bigr]d^2q, \tag{29}$$

since

$$\partial_{q_x}f^{\pm}(t,\mathbf{q}) = -\bigl(f^{\pm}(t,\mathbf{q}) - f^{\pm 2}(t,\mathbf{q})\bigr)v^{\pm}\hbar/(k_{\mathrm{B}}T),$$

and the contour integral vanishes. Indeed, when transferring the operator ∂_{q_x} from $v_x^{\pm}$ to $f^{\pm}(t,\mathbf{q})$ a substitution $q_x = \pm 2\pi/(\sqrt{3}a)$ occurs when integrating in the rectangular part of ZB (Fig. 1, *b*). It gives zero due to the periodicity. What remains is the contour integral corresponding to the triangular part

$$2\int\limits_{2\pi/(3a)}^{4\pi/(3a)}\bigl[v_x^{\pm}(t,q_x,q_y)f^{\pm}(t,q_x,q_y) - v_x^{\pm}(t,-q_x,q_y) \times f^{\pm}(t,-q_x,q_y)\bigr]dq_y.$$

We have $v_x^{\pm}(t,\pm q_x,q_y) = 0$ at $q_y = \pi/a$. By substituting $q_y' = q_y - \pi/a$, we get the intergal

$$2\int\limits_{-\pi/(3a)}^{\pi/(3a)} v_x^{\pm}(t,q_x,q_y')\bigl[f^{\pm}(t,q_x,q_y') + f^{\pm}(t,-q_x,q_y')\bigr]dq_y'.$$

In it $v_x^{\pm}(t,q_x,q_y')$ — is an odd function q_y', and q_x — function q_y'. For $t = 0$, the function in parentheses is even, so the integral is zero. Using q_0 expansions, it is also easy to prove this statement. Thus, the second part of the formula (4) is given by the integral (29).

Integration in BZ will be performed as follows. Let's designate the integral in a triangle 1, (Fig. 1, *b*) as $I_1\big(A_x(t)\big)$. Since $q_y = \sqrt{3}q_x/2$ on the line $\Gamma-\mathbf{K}$, is equal

$$I_1\big(A_x(t)\big) = \int\limits_0^{2\pi/(\sqrt{3}a)} dq_x \left(\int\limits_0^{\sqrt{3}q_x/2} f\big(\mathbf{q}, A_x(t)\big) dq_y \right),$$

where $F\big(\mathbf{q}, A_x(t)\big)$ — some function related to w and its derivatives. Due to the parity of q_y, the same integral will be on the triangle below the first one. On the two triangles with a mirror like reflection from y axis two integrals will give $2I_1\big(-A_x(t)\big)$. The integral $I_2\big(A_x(t)\big)$ over the second triangle 2 is also determined taking into account the dependence $q_y = -\sqrt{3}q_x/2$ in the form

$$I_2\big(A_x(t)\big) = \int\limits_0^{2\pi/(3a)} dq_y \left(\int\limits_0^{-\sqrt{3}q_x/2} f\big(\mathbf{q}, A_x(t)\big) dq_x \right).$$

It also shall be doubled. Similarly, the integral over triangle 3 with vertices $(\mathbf{K}', \mathbf{K}, (0, q_y))$ is defined taking into account $q_y = 4\pi/(3a) - \sqrt{3}q_x/2$. In the integrals over the areas reflected from the y axis, the sign of A_x should be changed. Finally, the complete integral over BZ is

$$I\big(A_x(t)\big) = 2\Big[I_1\big(A_x(t)\big) + I_1\big(-A_x(t)\big) + I_2\big(A_x(t)\big) + I_2\big(-A_x(t)\big) + I_3\big(A_x(t)\big) + I_3\big(-A_x(t)\big)\Big].$$

If there's no any pertubation, then $I(0) = 4[I_1(0) + I_2(0) + I_3(0)]$. A simpler approach to integration is to use the shooting method. Let's denote the function $z(x) = 4\pi/(3a) - |x|/\sqrt{3}$. In the double cycle with steps Δq_x and Δq_y over the area $-2\pi/(\sqrt{3}a) < q_x < 2\pi/(\sqrt{3}a)$, $-4\pi/(3a) < q_y < 4\pi/(3a)$ we consider only those points which satisfy the inequality $|q_y| < z(q_x)$. Only these points belong to the BZ. The result should be multiplied by the ratio of the number of counted points to their total number and by $\Delta q_x \Delta q_y$.

To determine the nonlinear response, consider the ratio (4). Let's take into account the expansions in $q_0(t)$. It is also possible to expand the mass. It is more convinient to take (4) given (30) in the form

$$j_x^{\pm}(t) = \frac{2e}{(2\pi)^2} \int\limits_{BZ} v_x^{\pm}(t, \mathbf{q}) f^{\pm}(t, \mathbf{q}) \times \left[\frac{q_0(t) v_x^{\pm}(t, \mathbf{q}) \hbar}{k_B T} \big(f^{\pm}(t, \mathbf{q}) - 1\big) - 1 \right] d^2q. \quad (30)$$

We will consider the electrons in the band gap, i.e. we take $j_x^+(t) = j_{x1}^+ q_0(t) + j_{x3}^+ q_0^3(t)$, where

$$j_{x1,3}^+ = \frac{2ev}{(2\pi)^2} \int\limits_{BZ} F_{1,3}^+(\mathbf{q}) d^2q,$$

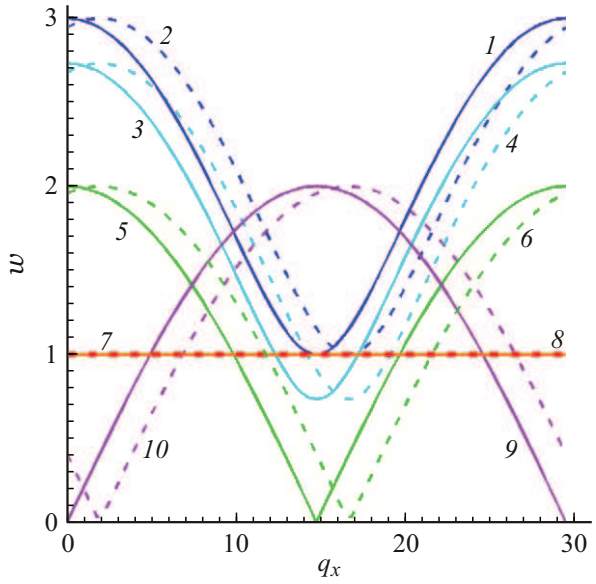

Figure 3. Dependence of the nonpertubated $w(\mathbf{q})$ (solid lines) and $w(t, \mathbf{q})$ (dashed lines) on q_x (1/nm) at $q_0 = 1.91\,\mathrm{nm}^{-1}$ ($A_x = 1$ A) and different q_y: $q_y = 0$ (curves *1,2*), $q_y = \pi/(3a)$ (*3,4*), $q_y = 2\pi/(3a)$ (*5,6*), $q_y = \pi/a$ (*7,8*), $q_y = 4\pi/(3a)$ (*9,10*). Range of values q_x: $\big(0, 4\pi/(\sqrt{3}a)\big)$, $\delta = 0$, $\varepsilon = 0$.

$$F_1^+(\mathbf{q}) = -\Big(v_0(\mathbf{q}) f_1^+(\mathbf{q}) + v_1(\mathbf{q}) f_0^+(\mathbf{q}) + v_0(\mathbf{q}) \frac{v_F \hbar}{k_B T} f_0^+(\mathbf{q}) \big(1 - f_0^+(\mathbf{q})\big) \Big),$$

$$F_3^+(\mathbf{q}) = -\big(v_0(\mathbf{q}) f_3^+(\mathbf{q}) + v_3(\mathbf{q}) f_0^+(\mathbf{q}) + v_1(\mathbf{q}) f_2^+(\mathbf{q}) + v_2(\mathbf{q}) f_1^+(\mathbf{q}) + v_1(\mathbf{q}) f_2^+(\mathbf{q}) \big) + v_0(\mathbf{q}) v_0(\mathbf{q}) f_2^+(\mathbf{q}) \frac{v_F \hbar}{k_B T} \times \big(f_0^+(\mathbf{q}) - 1\big) + v_0(\mathbf{q}) v_1(\mathbf{q}) f_1^+(\mathbf{q}) \frac{v_F \hbar}{k_B T} \big(f_0^+(\mathbf{q}) - 1\big) + 2v_0(\mathbf{q}) \times v(\mathbf{q}) f_1^+(\mathbf{q}) f_0^+(\mathbf{q}) \frac{v_F \hbar}{k_B T} + v_0(\mathbf{q}) v_0(\mathbf{q}) f_2^+(\mathbf{q}) f_0^+(\mathbf{q}) \frac{v_F \hbar}{k_B T}.$$

The third harmonic generation coefficient can now be estimated as $\kappa_{13} = e^2 E_0^2 \, |j_{x3}^+ / j_{x1}^+| / (\hbar^2 \omega_0^2)$.

Fig. 2 shows the analysis of m_{xx} component in VB (see Appendix, formula (A.15)). Fig. 3 illustrates the analysis of BZ, and Fig. 4 — shows x-component of the velocity. Their distortions under the action of the vector potential are shown. The value q_x varies from the center of BZ to the center of adjacent BZ. The values of mass and velocity in the subbands differ in signs, since $E(\mathbf{q}) = \pm\gamma_0 w(\mathbf{q})$. The effective mass component, according to the formula (A15), has poles corresponding to the spikes in Fig.2. From Dirac points in their small vicinity, the mass changes from zero according to a linear law. In the center of the valence band the effective mass is positive and scalar $m^* = 2\hbar/(\gamma_0 a^2) = 0.834 m_e$, and in the center of the band gap $m^* = -0.834 m_e$. The negative effective mass in the VB

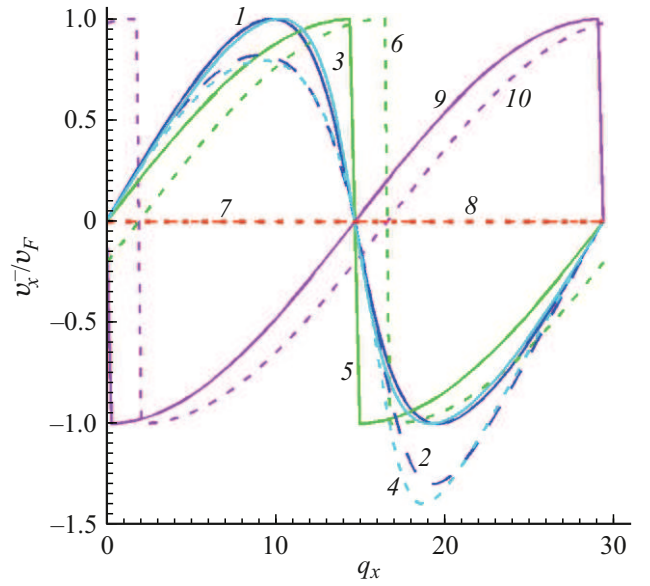

Figure 4. Normalized velocity component $v_x^-(\mathbf{q})/v_F$ (solid lines) and $v_x^-(t,\mathbf{q})/v_F$ (dashed lines) versus q_x (1/nm) at $q_0 = 1.91\,\text{nm}^{-1}$ ($A_x = 1\,\text{A}$) and different q_y: $q_y = 0$ (curves *1*), $q_y = \pi/(3a)$ (*2*), $q_y = 2\pi/(3a)$ (*3*), $q_y = \pi/a$ (*4*), $q_y = 4\pi/(3a)$ (*5*). Range of values q_x: $\left(0, 4\pi/(\sqrt{3}a)\right)$, $\delta = 0$, $\varepsilon = 0$.

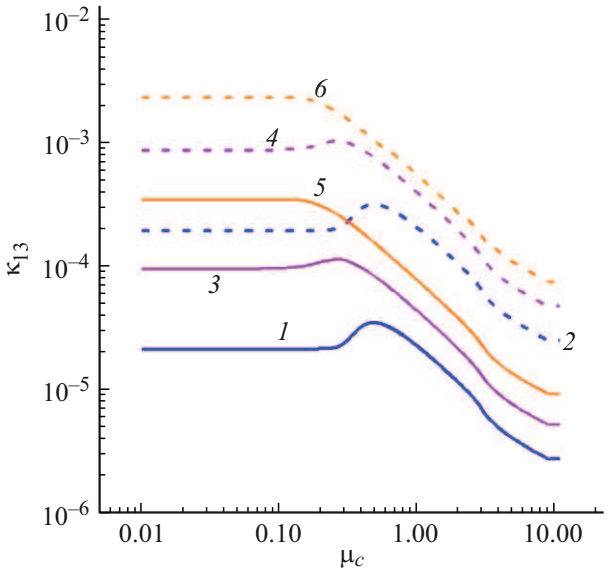

Figure 5. Dependence of κ_{13} on the chemical potential μ_c (eV) for different frequencies (THz), field amplitudes (V/m) and slit ε (eV): $\omega_0 = 10$, $E_0 = 10^4$, $\varepsilon = 0.3$ (curve *1*); $\omega_0 = 3.3$, $E_0 = 10^4$, $\varepsilon = 0.3$ (*2*); $\omega_0 = 10$, $E_0 = 10^4$, $\varepsilon = 0.16$ (*3*); $\omega_0 = 3.3$, $E_0 = 10^4$, $\varepsilon = 0.16$ (*4*); $\omega_0 = 10$, $E_0 = 10^4$, $\varepsilon = 0.095$ (curve *5*); $\omega_0 = 10$, $E_0 = 3.3 \cdot 10^4$, $\varepsilon = 0.095$ (*6*).

corresponds to a change in the curvature of the dispersion and means the opposite movement of the hole in the valence band, as it is usually interpreted in the theory of semiconductors. Fig. 5 illustrates the calculation of coefficient κ_{13}. Obtaining large values of the chemical potential requires doping, or the application of an external field, for which graphene is conveniently placed on a metallized substrate. This leads to an increase in the nonlinear response in the reflected wave. For room temperature and undoped graphene, the effect of temperature leads to a concentration $n_e(T) = \pi(k_B T)^2/(6\hbar^2 v_F^2) \approx 0.8 \cdot 10^{15}\,\text{m}^{-2}$ [16]. Given $\mu_c = (\hbar v_F)\sqrt{\pi n_e/2}$ we find $\mu_c = 0.023\,\text{eV}$, and for $E_0 = 10^6\,\text{V/m}$, $\omega_0 = 10^{13}\,\text{Hz}$ we get $\kappa_{13} = 1.6 \cdot 10^{-3}$, which is compliant with the experiments in [37,38]. Using it and its refinement over (28), we get the correction $\kappa_{13} = 1.71 \cdot 10^{-3}$. It is necessary to solve KBE for the time domain for strongly nonstationary processes.

Conclusion

To model transport processes in graphene, BZ is often used in the form of Dirac cones [20–36]. We should also mention the drawbacks of these methods. In fact, the cones do not have round, but triangular (with smoothed corners) sections (Fig. 1, *b*), and for energies greater than 1 eV, they turn into a curved surface of the Brillouin zone center. In [29], the replacement of the quasi-momentum $\mathbf{p} \to \mathbf{p} - \eta_0 e\mathbf{A}/c$ is used for the nonstationary Dirac equation with a linear vector potential in time $\mathbf{A}$, i.e. with a constant electric field in time. The static fields where the bonds in graphene are destructed have quite high values of 10^{10} V/m. Yet, in the fields that are about 2–3 order less the BZ has a significant distortion (see below). In harmonic fields, charge carriers oscillate and accelerate only for half a period, i.e., their range decreases significantly with increasing frequency inversely proportional to the square of the frequency. At that $\mathbf{E}(\omega) \sim \omega\mathbf{A}(\omega)$. The use of the linear dispersion $E(\tilde{\mathbf{q}}) = \pm|\tilde{\mathbf{p}}|v_F$ instead of $E(\mathbf{q}) = \pm\gamma_0 w(\mathbf{q})$ in these studies implies that the quasi-particles are located only in very small neighborhoods of Dirac cones (two valleys). Estimating the number of electrons at zero temperature in the high-voltage circuit based on DOS $D(E) = g_s g_v |E|/(2\pi\hbar^2 v_F^2)$ gives a value of [16] $n_e^{(0)} = 9\gamma_0^2/(\pi\hbar^2 v_F^2)$ 1.6 times greater than $n_0 = 3.8 \cdot 10^{19}\,1/\text{m}^2$ (corresponding to two π-electrons per graphene hexagon S_0). This is because of the linear approximation D (arrow in Fig. 1, *c*) in the linear dispersion approximation. A distribution of the type Fig. 1, *c* is obtained, in particular, by the method of density functional theory. Thus, the valley degeneracy $g_v = 2$ leads to higher values of DOS. This suggests that it is advisable to build models using the entire Brillouin zone. In numerous studies, nonlinear properties have been investigated experimentally [37–50]. In [51], a general quantum theory of nonlinear local dynamic conduction of the third order for linear dispersion is developed. In [52], the phenomenological relaxation parameters for third-order optical nonlinearity in doped graphene were investigated by solving the Bloch equation at Dirac points based on perturbation theory. The generation of odd harmonics has been theoretically and experimentally discovered in many studies. In the experiments [40,47] the

theoretical analysis was also made. A significant number of studies were focused on phenomenological nonlinear models (see [40,52–54]). As a rule, they define the nonlinear conductivity $\sigma(\omega) = \sigma_1(\omega) + \sigma_3(\omega)|\mathbf{E}(x, y, t)|^2$ with the response $\mathbf{J}(t) = \sigma(\omega)\mathbf{E}(x, y, t)$ and solve boundary value problems. In particular, the optical range uses the $\sigma_3(\omega) = 9ie^4v_F^2/(32\omega^4\hbar^3)$ value obtained in [40]. The nonlinear equation of motion for momentum and KBE is solved. A similar value for the THz band is given in [52]: $\sigma_3(\omega) = 3ie^4v_F^2/(32\omega^3\hbar^2\mu_c)$. It should be underscored that spectral and temporal representations are often used simultaneously, whereas in the time domain strict coupling should be integral.

In this paper, we demonstrate the possibility of solving the problem of nonlinear graphene response in the classical approach using integration over the entire Brillouin zone while taking into account tensor nonzero effective masses of quasiparticles in the strong coupling model [1]. The method allows using linear dispersion if an energy gap is introduced into the remote control, while the mass will no longer be strictly zero, but small. Actually, this method is a pertubation theory method. Without using small parameter expansions, the method is also applicable, but it is necessary to solve equations in the time domain. The pertubation method is applicable up to the fields of 10^7 V/m. With stronger fields, it is necessary to solve equations in the time domain and proceed from the first principles of calculations. Apparently, restrictions arise for the fields of 10^8-10^9 V/m. The solution can be generalized to arbitrary polarization.

The dielectric substrate makes it possible to enhance harmonic generation. Since the harmonic amplitudes are small, it is possible to solve the problem in a linear monochromatic approximation. Then the reflection coefficient is $R(\omega) = \big(1-Y(\omega)\big)/\big(1+Y(\omega)\big)$, where the normalized input conductivity on graphene is

$$Y(\omega) = \sqrt{\varepsilon}\,\frac{1 + i\sqrt{\varepsilon}\tan(k_0 d\sqrt{\varepsilon})}{\sqrt{\varepsilon} + i\tan(k_0 d\sqrt{\varepsilon})} + \eta_0\sigma(\omega).$$

There is a simple equivalent circuit for it, it is easy to determine the transmission coefficient $T(\omega)$ and the density $J(\omega)$, as well as the absorbed power.

$$P = \mathrm{Re}\big(J^2(\omega)/\sigma(\omega)\big)/2$$
$$= \sigma'(\omega)E_0^2\big(1 - |R^2(\omega)|^2 - |T^2(\omega)|^2\big)/2.$$

The substrate thickness d shall be selected based on the maximum condition P. However, due to the low conductivity of graphene, it is possible to approximate $k_0 d\sqrt{\varepsilon} = \pi/2$. In this case $Y(\omega) \approx \varepsilon$, and with large permittivity $R(\omega) \approx -1$. This structure creates harmonics mainly in the reflected field. By metallizing the substrate and applying a potential to graphene, it is possible to change μ_c and control the nonlinearity.

Funding

The study was supported by the Ministry of Science and Higher Education of the Russian Federation under the state assignment (project № SRR-2026-0006).

Conflict of interest

The author declares that he has no conflict of interest.

References

[1] P.R. Wallace. Phys. Rev. **71**, 622 (1947). DOI: 10.1103/PhysRev.71.622
[2] T. Ando. J. Phys. Society Jpn., **74** (3), 777 (2005). DOI: 10.1143/jpsj
[3] R. Saito, G. Dresselhaus, M.S. Dresselhaus. *Physical Properties of Carbon Nanotubes* (Imperial College Press, London, UK, 1998)
[4] G. Lovat, G.W. Hanson, R. Araneo, P. Burghignoli. Phys. Rev. B, **87**, 115429 (2013). DOI: 10.1103/PhysRevB.87.115429
[5] A.H. Castro Neto, F. Guinea, N.M.R. Peres, K.S. Novoselov, A.K. Geim. Rev. Mod. Phys., **81**, 109 (2009). DOI: 10.1103/RevModPhys.81.109
[6] S. Das Sarma, S. Adam, E.H. Hwang, E. Rossi. Rev. Mod. Phys., **83** (2), 407 (2011). DOI: 10.1103/RevModPhys.83.407
[7] G.W. Hanson. J. Appl. Phys., **103**, 064302 (2008). DOI: 10.1063/1.2891452
[8] L.A. Falkovsky, A.A. Varlamov. Eur. Phys. J. B, **56**, 281 (2007). DOI: 10.1140/epjb/e2007-00142-3
[9] L.A. Falkovsky. OpticJ. Phys. Conf. Ser., **129** (1), 012004 (2008). DOI: 10.1088/1742-6596/129/1/012004
[10] L.A. Falkovsky, S.S. Pershoguba. Phys. Rev. B, **76** (15), 153410 (2007). DOI: 10.1103/PhysRevB.76.153410
[11] L.A. Falkovsky. Phys. Usp., **55**, 1140 (2012). DOI: 10.3367/UFNe.0182.201211i.1223
[12] L.A. Falkovsky. Phys. Usp., **51**, 887 (2008). DOI: 10.1070/PU2008v051n09ABEH006625
[13] A.K. Geim, K.S. Novoselov. Nat. Mater, **6**, 183 (2007). DOI: 10.1038/nmat1849
[14] V.P. Gusynin, S.G. Sharapov, J.P. Carbotte. Int. J. Mod. Phys. B, **21**, 4611 (2007). DOI: 10.1142/S0217979207038022
[15] S. Reich, J. Maultzsch, C. Thomsen. Phys. Rev. B, **669**, 035412 (2002). DOI: 10.1103/PhysRevB.66.035412
[16] T. Fang, A. Konar, H. Xing, D. Jena. Appl. Phys. Lett., **91**, 092109 (2007). DOI: 10.1063/1.2776887
[17] N.N. Rozanov, *Nelineinaya optika. Part I. Uravneniya rasprostraneniya izlucheniya i nelineyniy otklik sredy* (SPb. State University Institute of Precision Mechanics and Optics, SPb, 2008)
[18] M.V. Davidovich. Tech. Phys., **69** (3), 265 (2024).
[19] M.V. Davidovich. Quant. Electron., **49** (9), 868 (2019). DOI: 10.1070/QEL16950
[20] S.A. Mikhailov. Europhys. Lett., **79**, 27002 (2007). DOI: 10.1209/0295-5075/79/27002
[21] M. Lewkowicz, B. Rosenstein. Phys. Rev. Lett., **102**, 106802 ((2009). DOI: 10.1103/PhysRevLett.102.106802
[22] B. Dora, R. Moessner. Phys. Rev. B, **81**, 165431 (2010). DOI: 10.1103/PhysRevB.81.165431
[23] B. Rosenstein, M. Lewkowicz, H.C. Kao, Y. Korniyenko. Phys. Rev. B, **81**, 041416(R) (2010). DOI: 10.1103/PhysRevB.81.041416

[24] M. Mecklenburg, J. Woo, B.C. Regan. Phys. Rev. B, **81**, 245401 (2010). DOI: 10.1103/PhysRevB.81.245401
[25] H.C. Kao, M. Lewkowicz, B. Rosenstein. Phys. Rev. B, **82**, 035406 (2010). DOI: 10.1103/PhysRevB.82.035406
[26] N. Vandecasteele, A. Barreiro, M. Lazzeri, A. Bachtold, F. Mauri. Phys. Rev. B, **82**, 045416 (2010). DOI: 10.1103/PhysRevB.82.045416
[27] M. Lewkowicz, H.-C. Kao, B. Rosenstein. Phys. Rev. B, **84**, 035414 (2011). DOI: 10.1103/PhysRevB.84.035414
[28] M.O. Goerbig. Rev. Mod. Phys., **83**, 1193 (2011). DOI: 10.1103/RevModPhys.83.1193
[29] S.P. Gavrilov, D.M. Gitman, N. Yokomizo. Phys. Rev. D, **86**, 125022 (2012). DOI: 10.1103/PhysRevD.86.125022
[30] N. Yokomizo. Ann. Phys., **351**, 166 (2014). DOI: 10.1016/j.aop.2014.08.024
[31] E. Barnes, E.H. Hwang, R. Throckmorton, S. Das Sarma. Phys. Rev. B, **89**, 235431 (2014). DOI: 10.1103/PhysRevB.89.235431
[32] S.A. Sato, H. Hirori, Y. Sanari, Y. Kanemitsu, A. Rubio. Phys. Rev. B, **103**, L041408 (2021). DOI: 10.1103/PhysRevB.103.L041408
[33] S.A. Smolyansky, A.D. Panferov, D.B. Blaschke, N.T. Gevorgyan. Particles, **2**, 208 (2019). DOI: 10.3390/particles2020015
[34] S.A. Smolyansky, D.B. Blaschke, V.V. Dmitriev, A.D. Panferov, N.T. Gevorgyan. Particles, **3**, 456 (2020). DOI: 10.3390/particles3020032
[35] S.P. Gavrilov, D.M. Gitman. Eur. Phys. J. Plus, **138**, 171 (2023). DOI: 10.1140/epjp/s13360-023-03786-9
[36] V.A. Tseryupa, D.V. Churochkin, V.V. Dmitriev, S.A. Smolyansky. ZhTF, **94** (3), 351 (2024) (in Russian). DOI: 10.61011/JTF.2024.03.57371.1-24
[37] T. Higuchi, C. Heide, K. Ullmann, H.B. Weber, P. Hommelhof. Nature, **550**, 224 (2017). DOI: 10.1038/nature23900
[38] H.A. Hafez, S. Kovalev, J.-C. Deinert, Z. Mics, B. Green, N. Awari, M. Chen, S. Germanskiy, U. Lehnert, J. Teichert, Z. Wang, K.-J. Tielrooij, Z. Liu, Z. Chen, A. Narita, K. Müllen, M. Bonn, M. Gensch, D. Turchinovich. Nature, **561**, 507 (2018). DOI: 10.1038/s41586-018-0508-1
[39] S. Kovalev, H.A. Hafez, K.-J. Tielrooij, J.-C. Deinert, I. Ilyakov, N. Awari, D. Alkaraz, K. Soundarapandian, D. Saleta, S. Germanskiy, M. Chen, M. Bawatna, B. Green, F.H.L. Koppens, M. Mittendorf, M. Bonn, M. Gensch, D. Turchinovich. Sci. Adv., **7**, eabf9809 (2021). DOI: 10.1126/sciadv.abf9809
[40] E. Hendry, P.J. Hale, J. Moger, A.K. Savchenko, S.A. Mikhailov. Phys. Rev. Lett., **105**, 097401 (2010). DOI: 10.1103/PhysRevLett.105.097401
[41] Z. Mics, K.-J. Tielrooij, K. Parvez, S.A. Jensen, I. Ivanov, X. Feng, K. Mullen, M. Bonn, D. Turchinovich. Nature Commun., **6**, 7655 (2015). DOI: 10.1038/ncomms8655
[42] N. Yoshikawa, T. Tamaya, K. Tanaka. Science, **356**, 736 (2017). DOI: 10.1126/science.aam8861
[43] I.V. Oladyshkin, S.B. Bodrov, Yu.A. Sergeev, A.I. Korytin, M.D. Tokman, A.N. Stepanov. Phys. Rev. B, **96**, 155401 (2017). DOI: 10.1103/PhysRevB.96.155401
[44] I.V. Oladyshkin, S.B. Bodrov, A.V. Korzhimanov, A.A. Murzanev, Yu.A. Sergeev, A.I. Korytin, M.D. Tokman, A.N. Stepanov. Phys. Rev. B, **106**, 205407 (2022). DOI: 10.1103/PhysRevB.106.205407
[45] C. Heide, T. Eckstein, T. Boolakee, C. Gerner, H.B. Weber, I. Franco, P. Hom-melhoff. Nano Lett., **21**, 9403 (2021). DOI: 10.1021/acs.nanolett.1c02538
[46] S. Cha, M. Kim, Y. Kim, S. Choi, S. Kang, H. Kim, S. Yoon, G. Moon, T. Kim, Y.W. Lee, G.Y. Cho, M.J. Park, C.-J. Kim, B.J. Kim, J.D. Lee, M.-H. Jo, J. Kim. Nature Commun., **13**, 6630 (2022). DOI: 10.1038/s41467-022-34337-y
[47] A.I. Berdyugin, N. Xin, H. Gao, S. Slizovskiy, Z. Dong, S. Bhattacharjee, P. Kumaravadivel, S. Xu, L.A. Ponomarenko, M. Holwill1, D.A. Bandurin, M. Kim, Y. Cao, M.T. Greenaway, K.S. Novoselov, I.V. Grigorieva, K. Watanabe, T. Taniguchi, V.I. Fal'ko, L.S. Levitov, R. Krishna Kumar, A.K. Geim. Science, **375** (6579), 430 (2022). DOI: 10.1126/science.abi8627
[48] A. Schmitt, P. Vallet, D. Mele, M. Rosticher, T. Taniguchi, K. Watanabe, E. Bocquillon, G. Féve, J.M. Berroir, C. Voisin, J. Cayssol, M.O. Goerbig, J. Troost, E. Baudin, B. Plaçais. Nature Phys., **19**, 830 (2023). DOI: 10.1038/s41567-023-01978-9
[49] K. Nakagawa, W. Mao, S.A. Sato, H. Ago, A. Rubio, Y. Kanemitsu, H. Hirori. APL Photon., **9**, 076107 (2024). DOI: 10.1063/5.0212022
[50] Y. Kim, M.J. Kim, S. Cha, S. Choi, C.-J. Kim, B.J. Kim, M.-H. Jo, J. Kim, J.D. Lee. Nano Lett., **24**, 1277 (2024). DOI: 10.1021/acs.nanolett.3c04278
[51] S.A. Mikhailov. Phys. Rev. B, **93**, 085403 (2016). DOI: 10.1103/PhysRevB.93.085403
[52] S.A. Mikhailov, K. Ziegler. J. Phys.: Condens. Matter, **20**, 384204 (2008). DOI: 10.1088/0953-8984/20/38/384204
[53] J.L. Cheng, N. Vermeulen, J.E. Sipe. Phys. Rev. B, **91**, 235320 (2015). DOI: 10.1103/PhysRevB.91.235320
[54] A. Pitilakis, D. Chatzidimitriou, E.E. Kriezis. Opt. Quant. Electron., **48**, 243 (2016). DOI: 10.1007/s11082-016-0510-5

Translated by T.Zorina

Appendix

Using dispersion (1) with substitution $q_x \to q_x - q_0(t)$, we have

$$w(t,\mathbf{q}) = w(\mathbf{q},q_0) = w(t,\mathbf{q}) = w(\mathbf{q}) + w_1(\mathbf{q})q_0(t) + w_2(\mathbf{q})q_0^2 q_0 + w_3(\mathbf{q})q_0^3 q_0 + \ldots, \tag{A1}$$

$$w_1(\mathbf{q}) = \frac{\sqrt{3}a}{w(\mathbf{q})}\sin\left(\sqrt{3}a\,\frac{q_x}{2}\right)\cos\left(\frac{q_y a}{2}\right), \tag{A2}$$

$$w_2(\mathbf{q}) = -\cos\left(\frac{q_y a}{2}\right) \times \frac{6a^2\cos\left(\frac{q_y a}{2}\right)\sin^2\left(\sqrt{3}a\frac{q_x}{2}\right) + w^2(\mathbf{q})\cos\left(\sqrt{3}a\frac{q_x}{2}\right)}{8w^3(\mathbf{q})} = \frac{\hbar^2}{2\gamma_0 m_{xx}}. \tag{A3}$$

$$w_3(\mathbf{q}) = \sqrt{3}a^3\cos\left(\frac{q_y a}{2}\right)\sin\left(\sqrt{3}a\,\frac{q_x}{2}\right) \times \frac{6a\cos\left(\frac{q_y a}{2}\right)\left[2\cos\left(\frac{q_y a}{2}\right)\sin^2\left(\sqrt{3}a\,\frac{q_x}{2}\right) + \cos\left(\sqrt{3}a\,\frac{q_x}{2}\right)\right] - w^4(\mathbf{q})}{8w^5(\mathbf{q})}. \tag{A4}$$

Functions w_1 and w_3 are odd functions over k_x, and function w_2 is even function. The functions are even over k_y. With a small disturbance q_0 away from the Dirac points w is a positive value. In the vicinity of the Dirac points $w_1(\mathbf{q}_\mathrm{D}) = 0$, since either the cosine or the sine become zero, whereas $w = 0$ is only at the points themselves, therefore the function (N1) is non-negative (Fig. 3). Adding a small value of ε (energy slit) to the root, we get a positive value of w.

To calculate the current density components, we use the group velocity in subbands

$$v_x^{\pm}(t,\mathbf{q}) = \pm\frac{\gamma_0}{\hbar}\,\partial_{q_x} w(t,\mathbf{q}) = \mp\frac{2v_F}{w(t,\mathbf{q})}\cos\left(\frac{q_y a}{2}\right) \times \sin\left(\sqrt{3}a\,\frac{q_x - q_0(t)}{2}\right),$$

where the sings are related to the subbands $\pi^{\pm}$. For the expansions we have

$$v_x^{\pm}(t,\mathbf{q}) = \mp v_F\big[v_0(\mathbf{q}) + v_1(\mathbf{q})q_0(t) + v_2(\mathbf{q})q_0^2(t) + v_3(\mathbf{q})q_0^3(t)\big], \tag{A5}$$

$$v_0(\mathbf{q}) = \frac{2\cos\left(a\,\frac{q_y}{2}\right)\sin\left(\sqrt{3}a\,\frac{q_x}{2}\right)}{w(\mathbf{q})}, \tag{A6}$$

$$v_1(\mathbf{q}) = \frac{2\cos\left(a\,\frac{q_y}{2}\right)\left[s_1 w(\mathbf{q}) - w_1(\mathbf{q})\sin\left(\sqrt{3}a\,\frac{q_x}{2}\right)\right]}{w^2(\mathbf{q})}, \tag{A7}$$

$$v_2(\mathbf{q}) = v_F \times \frac{2\cos\left(\frac{q_y a}{2}\right)\left[s_2 w(\mathbf{q}) - s_1 w_1(\mathbf{q}) - \sin\left(\frac{q_x\sqrt{3}a}{2}\right)\left(w_2(\mathbf{q}) - \frac{w_1^2(\mathbf{q})}{w(\mathbf{q})}\right)\right]}{w^2(\mathbf{q})}, \tag{A8}$$

$$v_3(\mathbf{q}) = \frac{2\cos\left(\frac{q_y a}{2}\right)\left[s_3 w(\mathbf{q}) - s_2 w_1(\mathbf{q}) - s_1\left(w_2(\mathbf{q}) - w_1^2(\mathbf{q})/w(\mathbf{q})\right) - \sin\left(\frac{q_x\sqrt{3}a}{2}\right)w_3(\mathbf{q})\right]}{w^2(\mathbf{q})}. \tag{A9}$$

Here,

$$s_1 = -(\sqrt{3}a/2)\cos(\sqrt{3}aq_x/2),$$
$$s_2 = -(3a^2/8)\sin(\sqrt{3}aq_x/2),$$
$$s_3 = (\sqrt{9}a^3/16)\cos(\sqrt{3}aq_x/2).$$

Functions v_0 and v_2 are odd over q_x, and functions v_1 and v_3 — are even. Over q_y all functions are even.

By expanding the exponent which enters DF

$$f^{\pm}(t,\mathbf{q}) = [1 + \exp(u_\pm + \delta_\pm)]^{-1}$$

we have

$$\exp(u_\pm + \delta_\pm) = \exp(u_\pm)[1 + \delta_\pm + \delta_\pm^2/2 + \delta_\pm^3/6],$$
$$u_\pm(\mathbf{q}) = \pm\left(\gamma_0 w(\mathbf{q}) - \mu_c\right)/(k_\mathrm{B}T),$$
$$u_\pm(\mathbf{q}) = \left(\pm\gamma_0 w(\mathbf{q}) - \mu_c\right)/(k_\mathrm{B}T),$$
$$\delta_\pm(t,\mathbf{q}) = \pm\gamma_0\left(w_1(\mathbf{q})q_0(t) + w_2(\mathbf{q})q_0^2(t) + w_3(\mathbf{q})q_0^3(t)\right)/(k_\mathrm{B}T), \tag{A10}$$

$$\exp(u_\pm + \delta_\pm) = \exp(u_\pm) \pm \frac{\gamma_0 w_1(\mathbf{q})}{k_\mathrm{B}T}\,q_0(t) + \left(\frac{\gamma_0^2 w_1^2(\mathbf{q})}{2(k_\mathrm{B}T)^2} \pm \frac{\gamma_0 w_2(\mathbf{q})}{k_\mathrm{B}T}\right)q_0^2(t) + \left(\frac{\gamma_0^2 2w_1(\mathbf{q})w_2(\mathbf{q})}{2(k_\mathrm{B}T)^2} \pm \frac{\gamma_0 w_3(\mathbf{q})q_0^3(t)}{k_\mathrm{B}T} + \frac{\gamma_0^3 w_1^2(\mathbf{q})}{6(k_\mathrm{B}T)^3}\right)q_0^3(t). \tag{A11}$$

Expanding the fraction, we get

$$f^{\pm}(t,\mathbf{q}) = f_0^{\pm}(\mathbf{q}) - f_0^{\pm^2}(\mathbf{q})\left(e_1^{\pm}(\mathbf{q})q_0(t) + e_2^{\pm}(\mathbf{q})q_0^2(t) + e_3^{\pm}(\mathbf{q})q_0^3(t)\right) + f_0^{\pm^3}(\mathbf{q})\left(e_1^{\pm^2}(\mathbf{q})q_0^2q_0^2(t) + 2e_1^{\pm}(\mathbf{q})e_2^{\pm}(\mathbf{q})q_0^3(t)\right) - f_0^{\pm^4}(\mathbf{q})e_1^{\pm^3}(\mathbf{q})q_0^3(t).$$

The DF expansion coefficients are indicated here

$$f^{\pm}(t,\mathbf{q}) = f_0^{\pm^{\pm}}(\mathbf{q}) + f_1^{\pm}(\mathbf{q})q_0 + f_2^{\pm}(\mathbf{q})q_0^2 + f_3^{\pm}(\mathbf{q})q_0^3, \tag{A12}$$

$$f_0^{\pm}(\mathbf{q}) = \frac{1}{1 + \exp(u_\pm)},$$
$$f_1^{\pm}(\mathbf{q}) = -f_0^{\pm^2}(\mathbf{q})e_1^{\pm}(\mathbf{q}),$$
$$f_2^{\pm}(\mathbf{q}) = -f_0^{\pm^2}(\mathbf{q})e_2^{\pm} + f_3^{\pm^3}(\mathbf{q})e_1^{\pm^2}, \tag{A13}$$
$$f_3^{\pm}(\mathbf{q}) = -f_0^{\pm^2}(\mathbf{q})e_3^{\pm}(\mathbf{q}) + 2f_0^{\pm^3}(\mathbf{q})e_1^{\pm}(\mathbf{q})e_2^{\pm}(\mathbf{q}) - f_0^{\pm^4}(\mathbf{q})e_1^{\pm^3}(\mathbf{q}),$$

the parity of which coincides with the parity of the indices, as well as the coefficients of the exponential expansion (A11):

$$e_1^{\pm}(\mathbf{q}) = \pm\frac{\gamma_0 w_1(\mathbf{q})}{k_\mathrm{B}T},$$
$$e_2^{\pm}(\mathbf{q}) = \left(\frac{\gamma_0^2 w_1^2(\mathbf{q})}{2(k_\mathrm{B}T)^2} \pm \frac{\gamma_0 w_2(\mathbf{q})}{k_\mathrm{B}T}\right), \tag{A14}$$
$$e_3^{\pm}(\mathbf{q}) = \left(\frac{\gamma_0^2 2w_1(\mathbf{q})w_2(\mathbf{q})}{2(k_\mathrm{B}T)^2} \pm \frac{\gamma_0 w_3(\mathbf{q})q_0^3(t)}{k_\mathrm{B}T} + \frac{\gamma_0^3 w_1^2(\mathbf{q})}{6(k_\mathrm{B}T)^3}\right).$$

For the diagonal component of the effective mass tensor used, we have

$$m_{xx}(\mathbf{q},t) = \frac{-\hbar^2 w^3(\mathbf{q},t)/(3\gamma_0 a^2)}{\cos\left(\frac{q_y a}{2}\right)\left[\cos\left(\frac{q_y a}{2}\right)\sin^2\left(\sqrt{3}a\,\frac{q_x - q_0(t)}{2}\right) + w^2(\mathbf{q},t)\cos\left(\sqrt{3}a\,\frac{q_x - q_0(t)}{2}\right)/2\right]}. \tag{A15}$$

It's required to expand its inverse value

$$m_{xx}^{-1}(\mathbf{q},t) = m_{xx}^{-1}(\mathbf{q}) + q_0(t)m_{xx1}^{-1}(\mathbf{q}) + q_0^2(t)m_{xx2}^{-1}(\mathbf{q}) + q_0^3(t)m_{xx3}^{-1}(\mathbf{q}),$$

however, we do not provide here this complex expansion, since it is more convenient to use the velocity expansion.